

Figure 1. Cryo-EM structures of ATTR184S fibrils from two patients, ATTR184S-1 (A-D) and ATTR184S-2 (E-H). A and E. Model reconstructions. The N terminal fragment of transthyretin is colored pink, and the C terminal is colored turquoise. B and F. 3D class averages. C and G. Atomic model of ATTR184S fibrils, as labeled. The N terminal fragment of transthyretin is colored pink, and the C terminal is colored turquoise. Arrows point at the mutation site. D and H. Close view of the cryo-EM density and atomic model of the polar channel in ATTR184S fibrils.

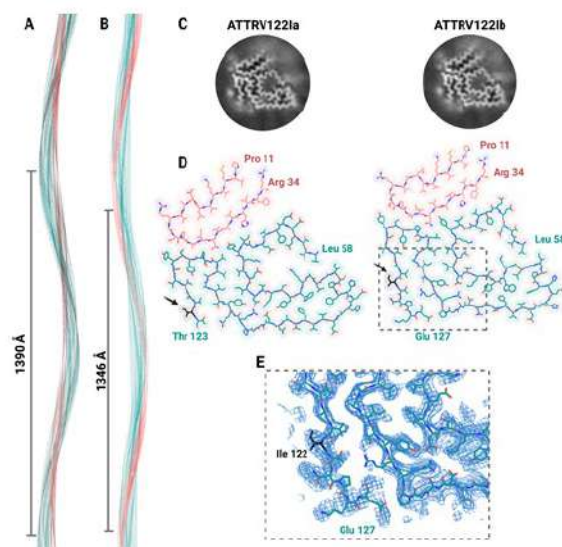


Figure 2. Cryo-EM structures of two distinct ATTRV122I fibrils extracted from the same patient. **A and B.** Model reconstructions of two distinct ATTRV122I fibrils from the same patients. They differ in the helical twist angle and crossover distance. **C.** 3D class averages of the two types of fibrils. **D.** Atomic model of ATTRV122I fibrils (Left, ATTRV122Ia; Right, ATTRV122Ib). The two fragments of transthyretin are colored pink (N terminus) and turquoise (C terminus). **E.** Enlarged view of the cryo-EM density and atomic model of the additional residues found in ATTRV122Ib fibrils.

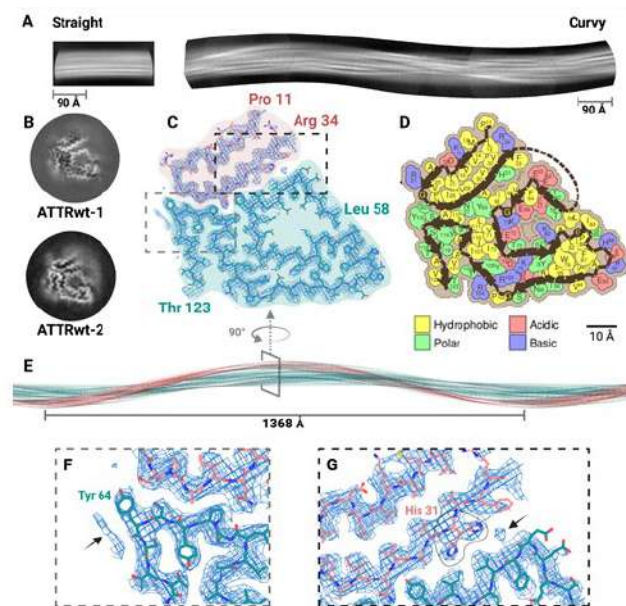


Figure 3. Cryo-EM structure of cardiac fibrils from an ATTRwt amyloidosis patient. **A.** Representative 2D class averages of straight fibrils (left) and curvy fibrils after stitching (right). **B.** 3D class averages of curvy fibrils from ATTRwt-1 and WTTRwt-2 patients. **C.** Cryo-EM density and atomic model of ATTRwt-1 fibrils. The model contains two fragments of transthyretin colored pink (residues Pro 11 to Arg 34) and turquoise (residues Leu 58 to Thr 123). **D.** Schematic view of the fibril core showing residue composition in patient ATTRwt-1. **E.** Model reconstruction of an ATTRwt-1 fibril. **F.** Close view of an unsatisfied density neighboring the residue Tyr 64 in ATTRwt-1 fibrils. **G.** Close view of the interface between the N and C terminal fragments, pointing to unsatisfied densities in ATTRwt-1 fibrils. One density blob could be assigned to an alternative rotamer of His 31 (dashed line).

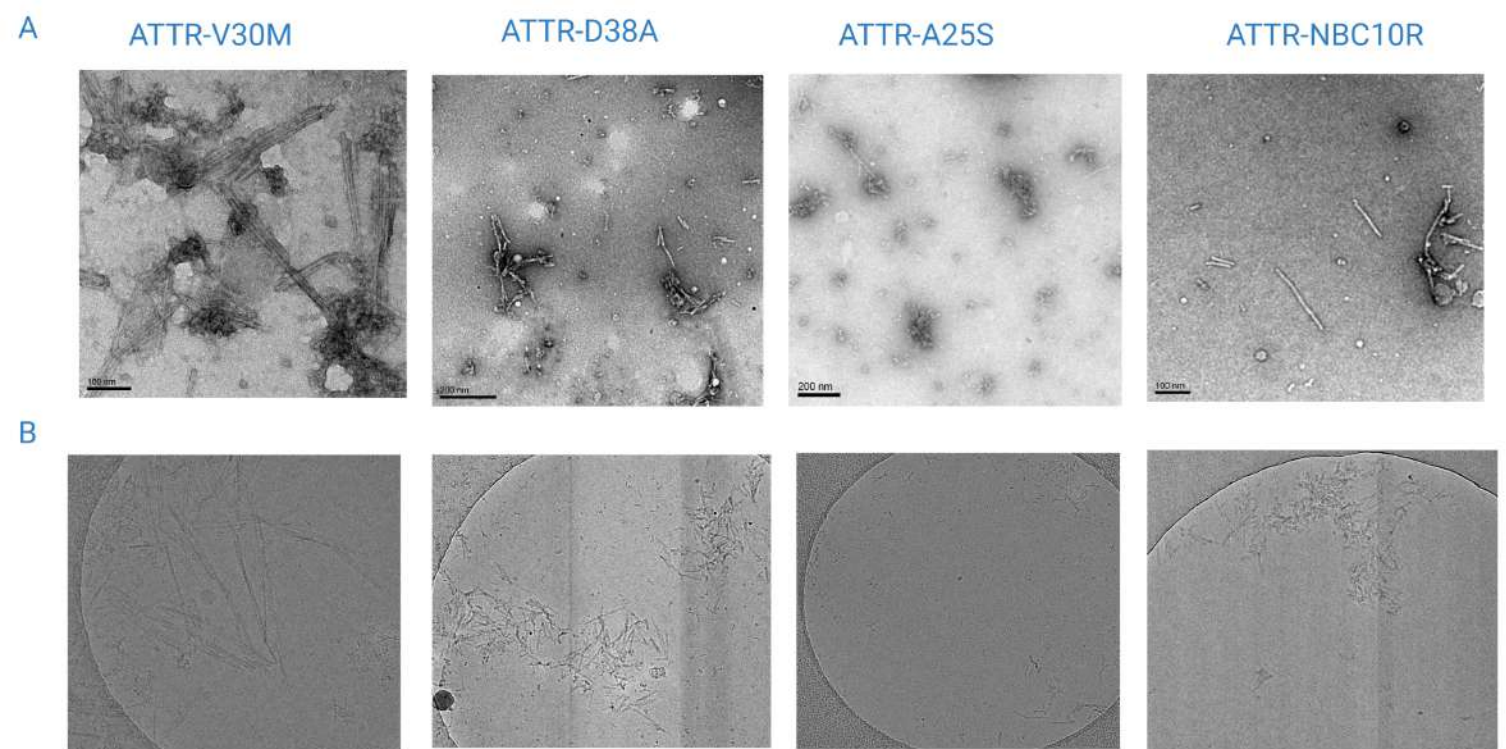


Figure 4. Electron-microscopy of ex-vivo fibrils extracted by the method of Schmidt et al. (6). We performed four fibrils extractions using the cardiac tissues of ATTR patients carrying familial mutations ATTR-V30M, ATTR-D38A, ATTR-A25S and ATTR-NBC10R. Amyloid fibril extraction was confirmed by negative staining EM (A) and cryo-EM of frozen grids at 45000X (B).